Supporting Information

Self-assembly strategy for synthesis of WO_3@TCN heterojunction: Efficient for photocatalytic degradation and hydrogen production via water splitting

Li Zhou, Wenjie Zhang, Zezhao Huang, Feng Hu, Peng Li *and Xiaoquan Yao *

Department of Applied Chemistry, School of Material Science and Technology, Nanjing University of Aeronautics and Astronautics, Nanjing 210016, P. R. China.

*Corresponding author：

E-mail addresses: yaoxq@nuaa.edu.cn (X. Yao), lpeng@nuaa.edu.cn (P. Li),

Table of Contents

Experimental section	Measurement and Characterization	S3
	DFT Theoretical Calculations	S4
Table S1.	Elemental content and ratios of samples	S5
Table S2	Specific surface area, pore size and pore volume data sheets	S5
Table S3	Comparison of photocatalytic degradation efficiency of tetracycline with 3%WO_3@TCN and other g-C_3N_4 samples	S5
Figure S1.	EDS elemental mapping images of 3%WO_3@TCN	S6
Figure S2.	Photoluminescence spectra of TCN and 3%WO_3@TCN	S7
Figure S3.	3%WO_3@TCN photocatalytic degradation of tetracycline in parallel experiments	S8
Figure S4.	Stability experiments of photocatalytic degradation of tetracycline of 3%WO_3@TCN	S9
Figure S5.	EPR spectra of DMPO-$^{\bullet}O_2^-$	S10
Figure S6.	Photocatalytic hydrogen evolution from water splitting on WO_3、TCN and 3%WO_3@TCN	S11
Reference		S12

Experimental section:

Measurement and Characterization

The crystal phase, photoelectric properties, elemental compositions, and morphologies were performed using an X-ray diffraction (XRD) spectroscope (Bruker D8 ADVANCE), UV–vis spectroscopy (JP Shimadzu Co., Ltd), scanning electron microscope (SEM) (Mira 4, Tescan) with energy-dispersed spectroscopy (EDS, Oxford Ultim Max65), and X-ray photoelectron spectroscopy (XPS) (250Xi, Thermo Fisher). Fourier transform infrared spectra (FT-IR) were analyzed by Thermo Scientific Nicolet iS20. The specific surface areas were determined with a surface area analyzer (ASAP 2020 Micropore System, Micromeritics Instrument Corporation, USA) by the Brunauer-Emmett-Teller (BET) method. The photo-generated charge carrier separation was recorded by Steady-state Photoluminescence (PL) spectra (Cray Eclipse, Varian, US).

DFT Theoretical Calculations

Based on the DFT theory, the figure of merit was calculated in this paper using the Vienna analog package (VASP) for first-principle DFT of composite photocatalysts. The truncation energy of the plane wave was set to 450 eV. In order to balance the geometry and optimize the lattice structure, the energy and force converged to 10^{-4} eV and 0.03 eV, respectively, with a K-point of 221. The crystal plane of WO_3 (010) and g-C_3N_4 (001) were selected for calculating. The P-space group was selected for WO_3 (a = 7.384 Å, b = 7.512 Å, and c = 3.846 Å), which corresponds to α = 90.00°, β = 90.00° , and γ = 90.00° to model the correlation. In addition, the crystal parameters of WO_3 and g-C_3N_4 materials were obtained from MDI Jade 6.5.

Table S1. Elemental Content and Ratios of Samples Obtained from Elemental Analysis and XPS Data

Catalysist	elemental content [a] (wt %)			
	C	**N**	**O**	**W**
TCN	45.39	54.61		
3%WO_3@TCN	43.02	54.06	2.84	0.08

[a] Elemental analysis results.

Table S2. Specific surface area, pore size and pore volume data sheets for samples

Catalysist	S_{BET}(m^2/g)	Pore diameter(nm)	Pore volume (cm^3/g)
WO_3	10.16	7.80	0.030
TCN	19.39	6.24	0.020
3% WO_3@TCN	26.51	8.15	0.053

Table S3. Comparison of photocatalytic degradation efficiency of tetracycline with 3%WO_3@TCN and other g-C_3N_4 samples

Catalyst	Dosage （mg）	Light source	Initial amount	Time （min）	Removal （%）
Mpg-C_3N_4-ZIF-8[1]	50	500W,Xe （λ≥ 420nm）	40 mg/L	180	74.8
Ag/g-C_3N_4[2]	50	300W, Xenon （λ≥ 420 nm）	20 mg/L	120	83
$BiVO_4$/g-C_3N_4[3]	20	300W, Xenon	20 mg/L	60	56
CeNCN[4]	10	300W, Xenon （λ≥420 nm）	10 mg/L	60	80.09
Tubular g-C_3N_4[5]	20	300W, Xenon （λ≥420 nm）	10 mg/L	60	50

3%WO_3@TCN	10	300W, Xenon （λ≥ 420 nm）	20 mg/L	80	86.5

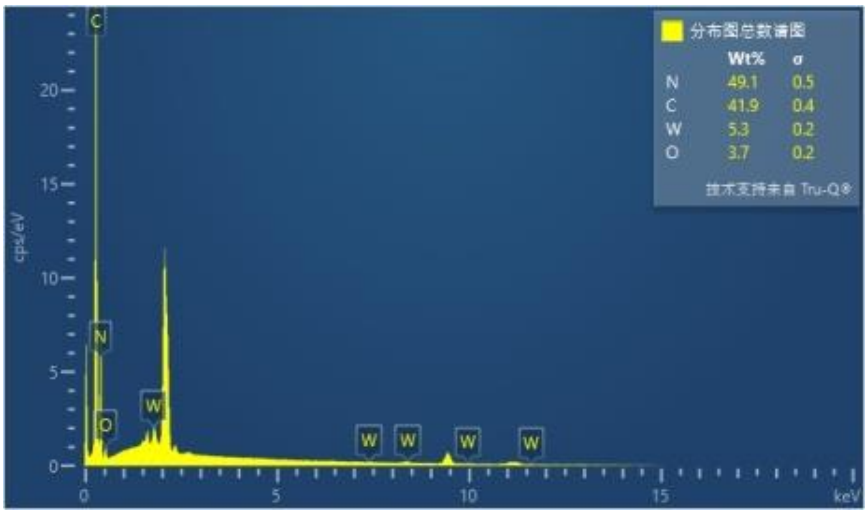


Figure S1. EDS elemental mapping images of 3%WO_3@TCN.

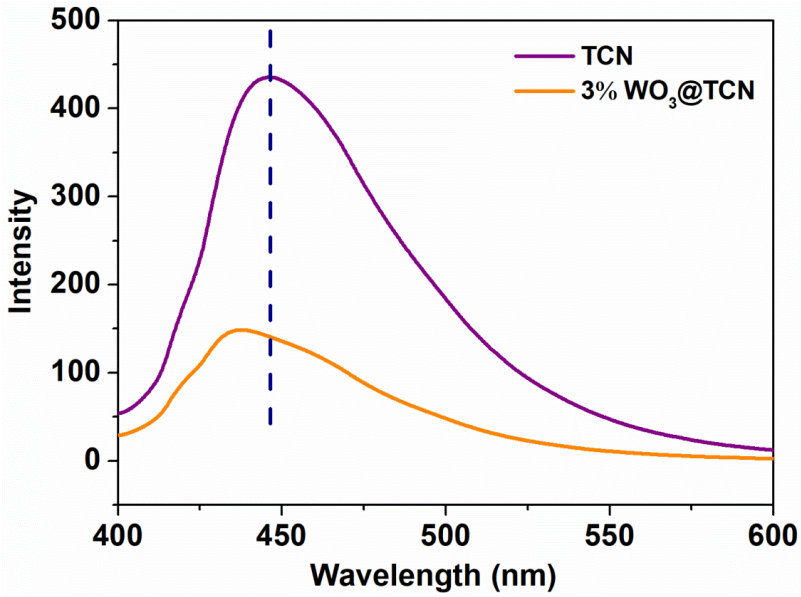


Figure S2. Photoluminescence spectra of TCN and 3%WO_3@TCN.

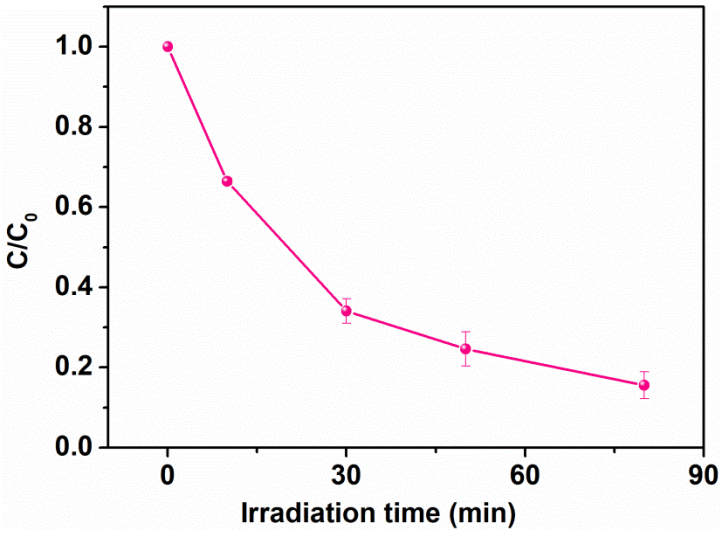


Figure S3. 3%WO_3@TCN photocatalytic degradation of tetracycline in parallel experiments

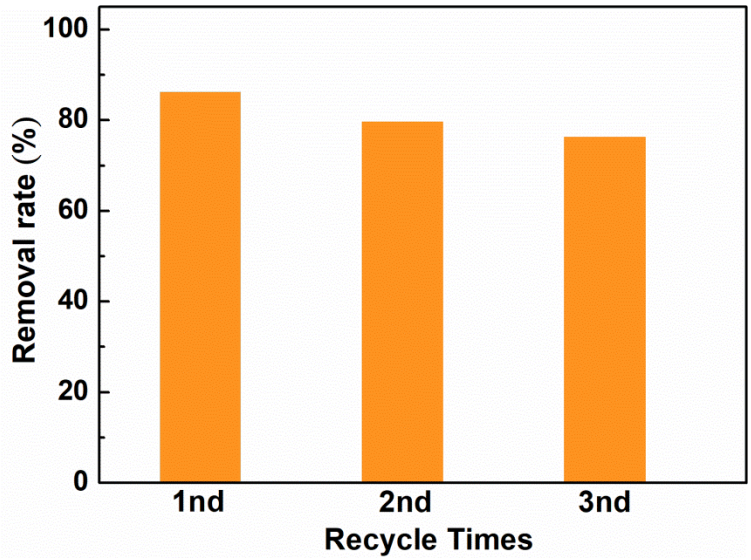


Figure S4. Stability experiments of photocatalytic degradation of tetracycline of 3%WO_3@TCN.

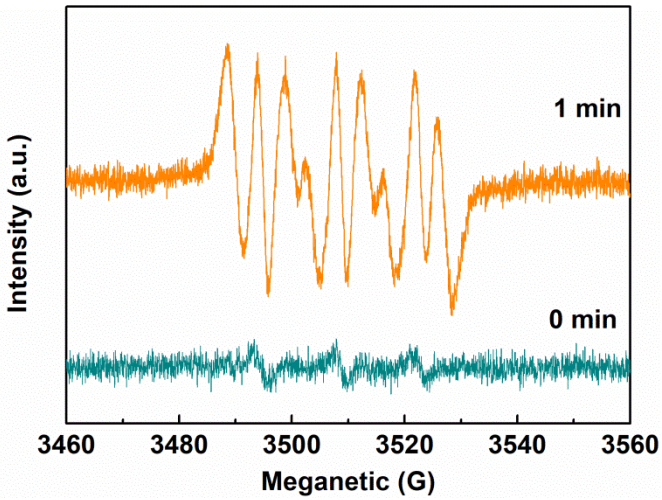


Figure S5. EPR spectra of DMPO-$^{\bullet}O_2^-$ in methanol dispersion in the presence of 3%WO_3@TCN

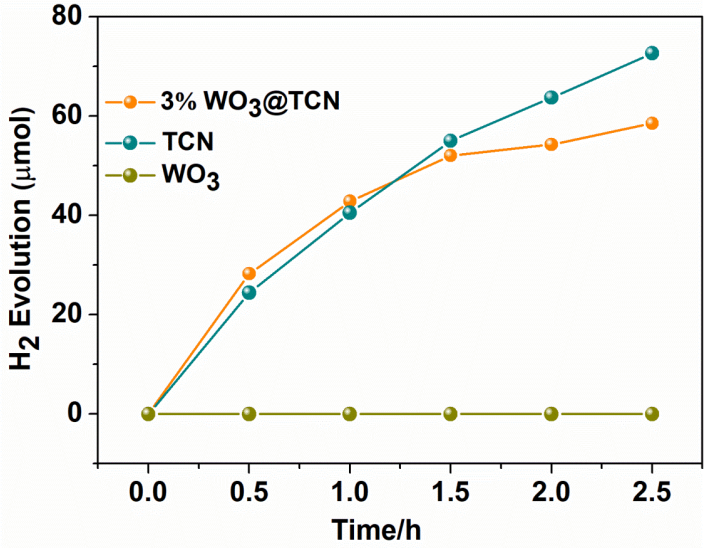


Figure S6. Photocatalytic hydrogen evolution from water splitting on WO_3、TCN and 3%WO_3@TCN with Pt as the cocatalyst and triethanolamine as the electron donor, under Xe lamp irradiation.

Reference

[1] Li D, Liu H, Niu C, et al. Mpg-C_3N_4-ZIF-8 composites for the degradation of tetracycline hydrochloride using visible light. Water Science Technology, 2019, 80(11): 2206-2217.

[2] Xu W, Lai S, Pillai S C, et al. Visible light photocatalytic degradation of tetracycline with porous Ag/graphite carbon nitride plasmonic composite: Degradation pathways and mechanism. Journal of Colloid and Interface Science, 2020, 574: 110-121.

[3] Zhang X, Xie X, Li J, et al. Type II heterojunction formed between 010 or 012 facets dominated bismuth vanadium oxide and carbon nitride to enhance the photocatalytic degradation of tetracycline. International Journal of Environmental Research and Public Health, 2022, 19(22): 14770.

[4] Xu F, An N, Lai C, et al. Nitrogen-doping coupled with cerium oxide loading co-modified graphitic carbon nitride for highly enhanced photocatalytic degradation of tetracycline under visible light. Chemosphere, 2022, 293: 133648.

[5] M Cao, J Zuo, Y Huang, Z Liu. Synthesis of tubular g-C_3N_4 via a H_2SO_4-assisted precursor self-assembly strategy for enhanced photocatalytic degradation of organic pollutant. Journal of Materials Science: Materials in Electronics, 2020, 31: 2022-2029.